Proceedings of the 17th
IEEE International Conference on Nanotechnology
Pittsburgh, USA, July 25-28, 2017

A Nanofluidics Study on Nanoscale Gas Bubble Defects in Dispensing-Based Nanoimprint Lithography*

Da Li, Xiaobai Ma, Nan Li, Rokbi Hossein, Wei Lu, Zhaoning Yu, Xiaogan Liang, *Member, IEEE*

Abstract— **Detrimental nanoscale gas bubble defects seriously hinder the practical applications of nanoimprint lithography in manufacturing of nanoelectronic devices. Here, we present a nanofluidics study on the formation and evolution mechanisms of nanoscale bubble defects in dispensing-based UV-curable nanoimprint lithography processes. Our work indicates that the formation of nanoscale bubble defects is mainly attributed to the pinning of resist spreading edges at the nanostructures or contaminants on the mold/substrate surfaces. Such pinning-induced nanoscale gas bubbles undergo an evolution process governed by the combinational effect of surface pinning and gas dissolution into resist. Such an evolution process results in a prominent drop of the gas pressure inside bubbles and therefore prevents nanoscale gas bubble defects from the complete dissolution into resists. This work identifies the critical mechanisms responsible for the formation of detrimental nanoscale bubble defects and provides important insights for the ultimate elimination of such defects.**

I. Introduction

Nanoimprint lithography (NIL) has shown the capability of patterning device structures smaller than 10 nm with a high throughput and a low processing cost.[1-3] One of the central goals in today's NIL research is to develop the processing methods that can improve NIL performance and yield, and to make NIL suitable for manufacturing commercially viable electronic, photonic, and magnetic device products. Among various NIL processes, UV-curable nanoimprint lithography (UV-NIL) based on in-situ liquid resist dispense and subsequent imprinting/curing steps has been adopted by the industry as an important candidate manufacturing technology for patterning nanoscale device features over large areas [3]. One major advantage of UV-NIL based on dispensable resists is that it does not need vacuum, which can greatly simplifies tool design. Especially, the vacuum operated overlay stage, a very costly module, is not needed by a dispensing-based NIL system. This advantage makes dispensing-based UV-NIL processes more suitable for high-throughput manufacturing in comparison with those based on spin-coated polymeric resists.[4] However, the current UV-NIL processes based on dispensable liquid resists still suffer seriously from gas bubble defects, which have significantly hindered the industrial applications associated with mass production of nanoelectronic devices [4-8]. There have been several previous works dedicated to identify the formation mechanisms of microscale bubble defects and explore the methods for removing such microscale bubbles through the gas dissolution into liquid resist [4, 8-10]. However, these previous works can hardly explain the long-term retention of nanoscale gas bubble defects in UV-NIL resists and the observed insolubility of such nanoscale bubbles in liquid resists.

Here, we present a nanofluidics study on the formation and evolution mechanisms of nanoscale bubble defects in UV-NIL. In particular, the interactions among nanofluidic resist flows, ambient gases, and mold/substrate surfaces are simulated using a FLUENT^{TM} computational fluidic dynamics (CFD) software package in combination with the dimensional analysis based on Buckingham PI theorem. This study has indicated that the formation of detrimental nanoscale bubble defects is attributed to the pinning of resist spreading edges at the topographical nanostructures or flat contaminants on the mold and substrate surfaces. Such pinning-induced nanoscale gas bubbles, after formation, undergo an evolution process governed by the net effect of pinning of triple-phase-lines and gas dissolution into the liquid resist. Such an evolution of nanoscale bubble defects results in a prominent drop of the gas pressure inside bubbles and therefore a significant reduction of the gas dissolution rate. Such a mechanism can explain the long-term retention of nanoscale gas bubble defects in UV-NIL resists.

II. Result and Analysis

In a dispensing-based UV-curable NIL process, a resist liquid is directly dropped or dispensed on a substrate in the form of discrete droplets through an inkjet system (Fig. 1 (a)). A mold (or template) is then implemented to press the resist droplet array into a thin film. During this process, the liquid resist flows and merges to eliminate the most ambient gas molecules between the mold (or the template) and the substrate (Fig. 1 (b)). However, it is expected that there are still a significant number of nanoscale gas bubbles trapped in the as-formed continuous resist film. After the mold press step, the trapped nanoscale bubbles are anticipated to

*Research supported by NSF (CMMI-1636132) and Seagate-University of Michigan Collaboration Project.

D. Li is now with the Mechanical Engineering Department, University of Michigan, Ann Arbor, MI 48109 USA (e-mail: dlihappy@umich.edu).
X. Ma is now with the Aerospace Engineering Department, University of Michigan, Ann Arbor, MI 48109 USA (e-mail: maxiaoba@umich.edu).
N. Li is now with the Mechanical Engineering Department, University of Michigan, Ann Arbor, MI 48109 USA (e-mail: cocolena@umich.edu).
R. Hossein is now with the Mechanical Engineering Department, University of Michigan, Ann Arbor, MI 48109 USA (e-mail: Rokni@umich.edu).
W. Lu is now with the Mechanical Engineering Department, University of Michigan, Ann Arbor, MI 48109 USA (e-mail: weilu@umich.edu).
Z. Yu is now with Seagate Technology PLC, Fremont, CA 94538 (e-mail: zhaoning.yu@seagate.com)
X. Liang is now with the Mechanical Engineering Department, University of Michigan, Ann Arbor, MI 48109 USA (e-mail: xiaoganl@umich.edu).

undergo an evolution process, finally relaxing to a final morphology that can prevent the bubbles from the complete dissolution into the liquid resist within the imprint process duration (Fig. 1 (c)). Finally, the liquid resist is cured by UV lights, leaving permanently trapped nanoscale bubble defects in the imprinted nanostructures.

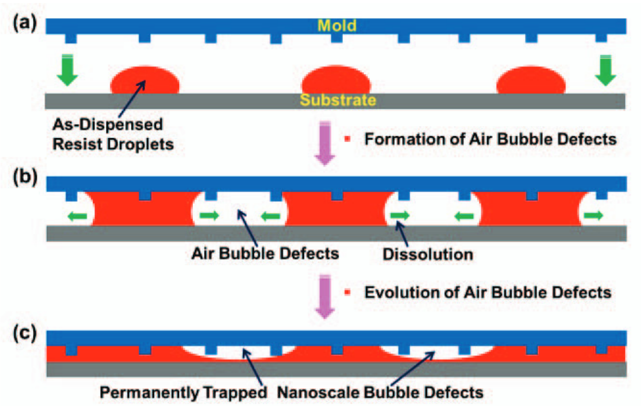

Figure 1. Schematic illustration of the formation and evolution of air bubble defects in a dispensing-based nanoimprint lithography process.

Figure 2 (a) displays the scanning electron microscope (SEM) images of typical nanoscale gas bubble defects formed in imprinted resist films. Such defects seriously degrade the yield of the desired functional nanostructures produced by UV-NIL processes. Even in case of the imprint process by using a flat mold without topographic nanostructures, such nanoscale bubble defects can be still formed in the resist film (Fig. 2 (b)). As shown in Fig. 2, all observed nanoscale gas bubble defects feature a shallow hemispherical shape (or bowl-like shape).

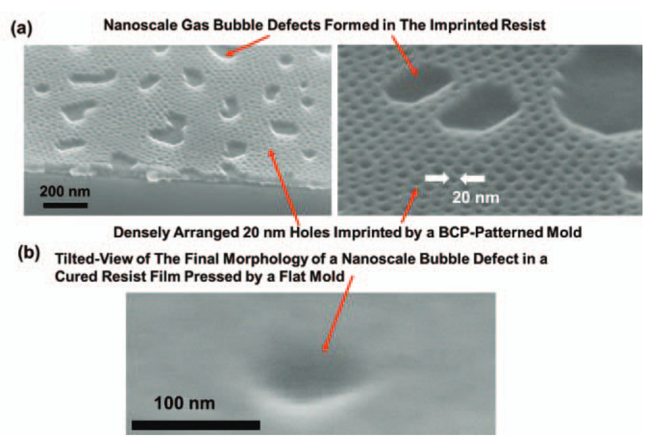

Figure 2. SEMs of (a) nanoscale gas bubble defects in a cured resist film (here, the densely arranged 20 nm holes are desirable structures imprinted by a mold that was fabricated using block-copolymer (BCP) self-assembly) and (b) tilted view of the final profile of a nanoscale bubble defect trapped in a resist film imprinted by a flat mold.

We performed a series of nanofluidics simulations, seeking to identify the most critical factors responsible for the formation of permanent nanoscale gas defects in UV-NIL processes. Our simulation models are constructed based on FLUENT™ computational fluidic dynamics (CFD) software in combination with the dimensional analysis based on Buckingham PI theorem, which can enable the simulation of nanoscale resist flows, gas bubble evolutions, as well as the interactions among resist, gas, and solid surfaces. Our work has strongly implied that the surface pinning of the spreading edges of resist droplets result in the nanoscale gas bubbles permanently trapped in the imprinted resist. More detailed results from this work are discussed as follow.

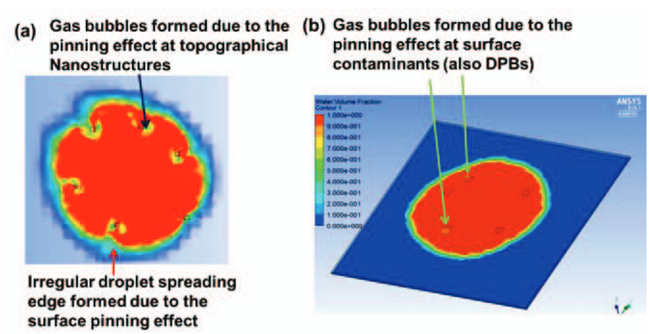

Figure 3. Nanofluidic simulation results of an individual spreading resist droplet on surfaces with randomly dispersed (a) topographical nanostructures and (b) flat surface contaminants (modeled as highly dewetting areas).

During a UV-NIL process, when a resist droplet is displaced by the mold and laterally spreading, a series of surface features can result in pinning effects to the spreading edges of the droplet and trap gas bubbles. Specifically, there are three sources of the pinning effects: (1) topographical nano/microstructures pre-fabricated on the mold and the substrate, (2) nanoscale particles (NPs) (NPs can be also regarded as randomly-distributed topographical nanostructures), and (3) hydrocarbon-based surface contaminants that usually results in pinning sites with highly dewetting areas for the resist liquids. Our nanofluidics simulation results show that all of these features result in very similar pinning effects to the resist flows. For example, Fig. 3 shows the simulation results of an individual spreading resist droplet (volume ~ 1 nL) on the surfaces with randomly dispersed (a) topographical NPs and (b) flat surface contaminants. The presence of such pinning features results in two effects: (1) the pinning of the resist spreading edge at NPs or contaminants can directly form nanoscale gas bubbles, which are termed as directly-pinned bubbles (DPBs); (2) the resist spreading edge becomes irregular after sweeping over the pinning sites, and the mergence of multiple such droplets can trap more gas bubbles, which are termed as mergence-induced bubbles (MIBs), as displayed in Fig. 4. It should be noted that the MIB effect is much less serious and more easily addressed in comparison with the DPB effect because of the following two reasons. (1) The pinning-induced irregularity (or roughness) of the resist spreading edge can be smoothed out by the surface tension of the resist. The relaxation time (τ) of this smoothing effect is expected to scale with the square root of the droplet volume ($V^{1/2}$). Therefore, the smaller resist droplet size (*e.g.*, 10-100 pL for a typical manufacturing-grade UV-NIL system) can result in a faster smoothing process so that the droplets subjected to pinning sites can quickly re-obtain a regular spreading edge before the inter-droplet mergence. (2) Most MIB defects are spatially away from the pinning sites, and they can be quickly dissolved into the resist liquid.[4] The following result and discussion will specifically explain the reason why the DPB defects trapped at pinning sites (topographical nanostructures, NPs, or surface contaminants) cannot be completely removed *via* the dissolution process. Such DPBs are permanently existing detrimental NIL defects.

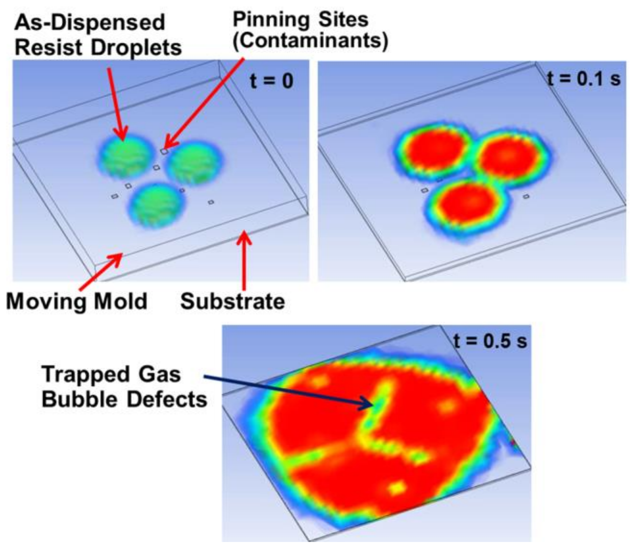

Figure 4. Time-dependent simulation (top-view) of displacement and mergence of multiple resist droplets on a contaminated substrate.

When a DPB defect is initially trapped at a pinning site (*e.g.*, a hydrocarbon contaminant), it has a relatively high internal gauge pressure *P* (or Laplace pressure) that can be approximately evaluated by Eqn. 1, where σ is the surface tension of the resist, *d* is the resist thickness, θ_m and θ_s are the contact angles of the resist spreading edges on the mold and the substrate, respectively.

$$P \approx \frac{\sigma(\cos(\theta_m)+\cos(\theta_s))}{d} \qquad \text{(Eqn. 1)}$$

Typically, both θ_m and θ_s are less than 100°, and *d* is in the range of 20 – 100 nm, which can result in a large Laplace pressure (*P*) of 0.5 – 3 MPa. This large Laplace pressure can result in the dissolution of gas molecules into the resist, shrinking the bubble. If no pinning site is presented, this dissolution process could remove a 100s nm size bubble defect in a few seconds [4]. However, our nanofluidics simulation results imply that, due to the pinning of the resist spreading edge on the contaminant, gas dissolution is anticipated to turn the initially disk-like bubble into a shallow hemispherical (or bowl-like) shape with a pinning angle θ_p >> 90°. More specifically, Fig. 5 displays the time-dependent simulation (2D cross-sectional view) result of the profile evolution of a gas bubble defect pinned at a contaminant region on the mold. Due to the pinning effect, the bubble finally has a hemispherical shape with significantly reduced Laplace pressure, which is consistent with the SEM-observed profile of typical real nanoscale gas defects in the cured resist, as shown in Fig. 2 (b). The Laplace pressure inside such a pinned nanoscale bubble can be estimated by using Eqn. 2, where *s* is the typical lateral size of a pinning region (0.5 to 1 μm).

$$P \approx 4\sigma \sin(\theta_p)/s \qquad \text{(Eqn. 2)}$$

The typical Laplace pressure inside such a pinned nanoscale bubble is estimated to be less than 0.05 MPa, which is at least one order of magnitude lower than that in a typical unpinned bubble. Accordingly, the gas dissolution rate for a pinned bubble is expected to be at least one order of magnitude lower [4]. During a manufacturing process, such a slow dissolution rate cannot completely eliminate DPB defects within the process time (typically 3-10 s).

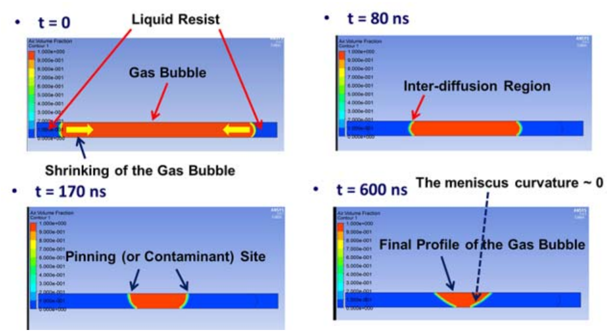

Figure 5. Time-dependent simulation (2D cross-sectional view) of the profile evolution of a gas bubble defect pinned at a contaminant region on the mold.

Finally, our nanofluidics simulation results also imply that when a nanoscale bubble is formed due to the pinning of the spreading resist edge at a nanostructure or contaminant area, additional smaller satellite bubbles could be formed along the spreading direction of the resist edge. More specifically, Fig. 6 (a) displays our result of the time-dependent simulation (top-view) of the trapping of a gas bubble defect around a nanoscale contaminant area. After this bubble is initially trapped, it is drawn into a long oval shape by the resist flow. The Rayleigh instability of such a long bubble usually breaks the bubble into several smaller satellite bubbles, and the arrangement of these satellite bubbles is expected to be along the spreading direction of the resist flow. Figure 6 (b) shows the SEM-observed satellite bubbles formed in the proximity of a nanoscale contaminant area on the substrate. The consistency between our simulation and experimental observation further support that the surface pinning of the spreading edges of resist droplets is responsible for the nanoscale gas bubbles permanently trapped in the imprinted resist.

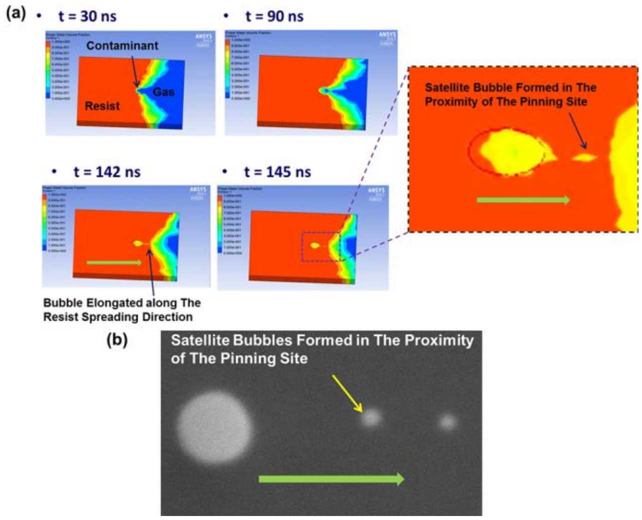

Figure 6. (a) Time-dependent simulation (top-view) of the trapping of gas bubble defects around a contaminant area and the formation of satellite bubbles along the spreading direction of the resist flow. (b) SEM of a set of representative satellite bubbles formed in the proximity of a pinning site.

III. CONCLUSION

In summary, we present a nanofluidics study on the formation and evolution mechanisms of nanoscale bubble defects in liquid UV-NIL resists. In this work, we have developed a nanofluidics simulation model capable of simulating the interactions among nanofluidic resist flows, ambient gases, and solid mold/substrate surfaces. The presented simulation model is constructed using a FLUENT^{TM} computational fluidic dynamics (CFD) software package in combination with the dimensional analysis based on Buckingham PI theorem. Our simulation results strongly implies that the formation of detrimental nanoscale bubble defects in UV-NIL is mainly attributed to the pinning of resist spreading edges at the topographical nanostructures or flat organic contaminants on the mold and substrate surfaces. Our simulation also implies that such pinning-induced nanoscale gas bubbles also undergo an evolution process governed by the net effect of pinning of triple-phase-lines and gas dissolution into the liquid resist. Such an evolution of nanoscale bubble defects results in a prominent drop of the gas pressure inside bubbles and therefore a significant reduction of the gas dissolution rate. Such a mechanism can explain the long-term retention of nanoscale gas bubble defects in UV-NIL resists. Finally, our simulation result is highly consistent with our experimental observation of nanoscale gas bubble defects in UV-NIL resists. This work has identified the critical mechanisms responsible for the formation of detrimental nanoscale bubble defects and provides important insights for the ultimate elimination of such defects. For example, new nanoimprint lithography tools with optimized control of nanofluidic resist flows are anticipated to be created and capable of minimizing the pinning events during the imprint processes.

ACKNOWLEDGMENT

The work is supported by the NSF grant # CMMI-1636132 and Seagate-University of Michigan Collaboration Project.

REFERENCES

[1] Chou, S.Y., Krauss, P.R., and Renstrom, P.J.: 'Imprint of Sub-25 nm Vias AND Trenches in Polymers', Appl. Phys. Lett., 1995, 67, (21), pp. 3114-3116

[2] Chou, S.Y., Krauss, P.R., and Renstrom, P.J.: 'Imprint lithography with 25-nanometer resolution', Science, 1996, 272, (5258), pp. 85-87

[3] Colburn, M., Johnson, S., Damle, S., Bailey, T., Choi, B., Wedlake, M., Michaelson, T., Sreenivasan, S.V., Ekerdt, J., and Willson, C.G., Proceedings of SPIE 1999 3676 pp. 379

[4] Liang, X.G., Tan, H., Fu, Z.L., and Chou, S.Y.: 'Air bubble formation and dissolution in dispensing nanoimprint lithography', Nanotechnology, 2007, 18, (2)

[5] Liang, X., Fu, Z., and Chou, S.Y.: 'Air bubble formation and dissolution in dispensing nanoimprint lithography ', The Fourth International Conference on Nanoimprint and Nanoprint Technology (NNT 2005) Oct. 19 – 21, 2005, Nara, Japan

[6] Liang, X., Fu, Z., and Chou, S.Y.: 'Further study on air dissolution in dispensing nanoimprint resists ', The 50th International Conference on Electron, Ion, Photon Beams and Nanolithography (EIPBN 2006) May 30 -- June 2, 2006, Baltimore, MD

[7] Liang, X., Tan, H., Fu, Z., and Chou, S.Y.: 'Effects of resist residual layer thickness on air dissolution in dispensing nanoimprint lithography ', The Fifth International Conference on Nanoimprint and Nanoprint Technology (NNT 2006) Nov. 15 – 18, 2006, San Francisco, CA

[8] Hiroshima, H., and Komuro, M.: 'Control of bubble defects in UV nanoimprint', Japanese Journal of Applied Physics Part 1-Regular Papers Brief Communications & Review Papers, 2007, 46, (9B), pp. 6391-6394

[9] Hiroshima, H., and Komuro, M.: 'UV-nanoimprint with the assistance of gas condensation at atmospheric environmental pressure', J Vac Sci Technol B, 2007, 25, (6), pp. 2333-2336

[10]Hiroshima, H., Komuro, M., Kasahara, N., Kurashima, Y., and Taniguchi, J.: 'Elimination of pattern defects of nanoimprint under atmospheric conditions', Jpn J Appl Phys 1, 2003, 42, (6B), pp. 3849-3853